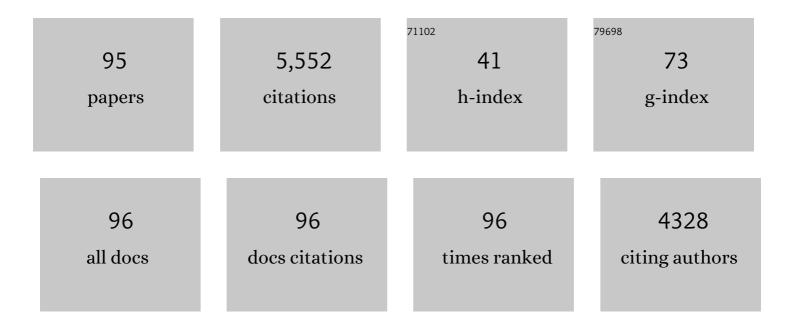
List of Publications by Year in descending order

Source: https://exaly.com/author-pdf/2061527/publications.pdf Version: 2024-02-01



IOHN P RADCAD

#	Article	IF	CITATIONS
1	Characterization of U(VI)-carbonato ternary complexes on hematite: EXAFS and electrophoretic mobility measurements. Geochimica Et Cosmochimica Acta, 2000, 64, 2737-2749.	3.9	320
2	Environmental Speciation of Actinides. Inorganic Chemistry, 2013, 52, 3510-3532.	4.0	318
3	Thermodynamically controlled preservation of organic carbon in floodplains. Nature Geoscience, 2017, 10, 415-419.	12.9	234
4	Non-uraninite Products of Microbial U(VI) Reduction. Environmental Science & Technology, 2010, 44, 9456-9462.	10.0	220
5	Spectroscopic Confirmation of Uranium(VI)â^'Carbonato Adsorption Complexes on Hematite. Environmental Science & Technology, 1999, 33, 2481-2484.	10.0	216
6	Bacteriogenic Manganese Oxides. Accounts of Chemical Research, 2010, 43, 2-9.	15.6	213
7	Adsorption of Uranium(VI) to Manganese Oxides: X-ray Absorption Spectroscopy and Surface Complexation Modeling. Environmental Science & Technology, 2013, 47, 850-858.	10.0	187
8	Uranium Isotope Fractionation during Adsorption to Mn-Oxyhydroxides. Environmental Science & Technology, 2011, 45, 1370-1375.	10.0	154
9	Uranium(IV) adsorption by natural organic matter in anoxic sediments. Proceedings of the National Academy of Sciences of the United States of America, 2017, 114, 711-716.	7.1	142
10	Persistence of uranium groundwater plumes: Contrasting mechanisms at two DOE sites in the groundwater–river interaction zone. Journal of Contaminant Hydrology, 2013, 147, 45-72.	3.3	136
11	Products of abiotic U(VI) reduction by biogenic magnetite and vivianite. Geochimica Et Cosmochimica Acta, 2011, 75, 2512-2528.	3.9	130
12	Structure of Biogenic Uraninite Produced by <i>Shewanella oneidensis</i> Strain MR-1. Environmental Science & Technology, 2008, 42, 7898-7904.	10.0	119
13	Bioremediation of uranium-contaminated groundwater: a systems approach to subsurface biogeochemistry. Current Opinion in Biotechnology, 2013, 24, 489-497.	6.6	119
14	Element release and reaction-induced porosity alteration during shale-hydraulic fracturing fluid interactions. Applied Geochemistry, 2017, 82, 47-62.	3.0	116
15	The product of microbial uranium reduction includes multiple species with U(Ⅳ)–phosphate coordination. Geochimica Et Cosmochimica Acta, 2014, 131, 115-127.	3.9	114
16	Structural characterization of terrestrial microbial Mn oxides from Pinal Creek, AZ. Geochimica Et Cosmochimica Acta, 2009, 73, 889-910.	3.9	112
17	Uranium speciation and stability after reductive immobilization in aquifer sediments. Geochimica Et Cosmochimica Acta, 2011, 75, 6497-6510.	3.9	112
18	Influence of Dynamical Conditions on the Reduction of U ^{VI} at the Magnetiteâ^'Solution Interface. Environmental Science & Technology, 2010, 44, 170-176.	10.0	110

#	Article	IF	CITATIONS
19	Quantitative Separation of Monomeric U(IV) from UO ₂ in Products of U(VI) Reduction. Environmental Science & Technology, 2012, 46, 6150-6157.	10.0	107
20	Impact of Organics and Carbonates on the Oxidation and Precipitation of Iron during Hydraulic Fracturing of Shale. Energy & Fuels, 2017, 31, 3643-3658.	5.1	104
21	Water Table Dynamics and Biogeochemical Cycling in a Shallow, Variably-Saturated Floodplain. Environmental Science & Technology, 2017, 51, 3307-3317.	10.0	100
22	Comparative dissolution kinetics of biogenic and chemogenic uraninite under oxidizing conditions in the presence of carbonate. Geochimica Et Cosmochimica Acta, 2009, 73, 6065-6083.	3.9	98
23	Reduction of U(VI) Incorporated in the Structure of Hematite. Environmental Science & Technology, 2012, 46, 9428-9436.	10.0	82
24	Relative Reactivity of Biogenic and Chemogenic Uraninite and Biogenic Noncrystalline U(IV). Environmental Science & Technology, 2013, 47, 9756-9763.	10.0	81
25	Biogeochemical Controls on the Product of Microbial U(VI) Reduction. Environmental Science & Technology, 2013, 47, 12351-12358.	10.0	79
26	Physico-Chemical Heterogeneity of Organic-Rich Sediments in the Rifle Aquifer, CO: Impact on Uranium Biogeochemistry. Environmental Science & Technology, 2016, 50, 46-53.	10.0	77
27	Probing the sorption reactivity of the edge surfaces in birnessite nanoparticles using nickel(II). Geochimica Et Cosmochimica Acta, 2015, 164, 191-204.	3.9	75
28	Reduction of Uranium(VI) by Soluble Iron(II) Conforms with Thermodynamic Predictions. Environmental Science & Technology, 2011, 45, 4718-4725.	10.0	70
29	In Situ Grazing-Incidence Extended X-ray Absorption Fine Structure Study of Pb(II) Chemisorption on Hematite (0001) and (1-102) Surfaces. Langmuir, 2004, 20, 1667-1673.	3.5	68
30	Oxidative Dissolution of Biogenic Uraninite in Groundwater at Old Rifle, CO. Environmental Science & Technology, 2011, 45, 8748-8754.	10.0	66
31	Copper sorption by the edge surfaces of synthetic birnessite nanoparticles. Chemical Geology, 2015, 396, 196-207.	3.3	64
32	Competing retention pathways of uranium upon reaction with Fe(II). Geochimica Et Cosmochimica Acta, 2014, 142, 166-185.	3.9	60
33	Evidence for multiple modes of uranium immobilization by an anaerobic bacterium. Geochimica Et Cosmochimica Acta, 2011, 75, 2684-2695.	3.9	56
34	Speciation and Reactivity of Uranium Products Formed during <i>in Situ</i> Bioremediation in a Shallow Alluvial Aquifer. Environmental Science & Technology, 2014, 48, 12842-12850.	10.0	56
35	Tetra- and Hexavalent Uranium Forms Bidentate-Mononuclear Complexes with Particulate Organic Matter in a Naturally Uranium-Enriched Peatland. Environmental Science & Technology, 2016, 50, 10465-10475.	10.0	55
36	Understanding controls on redox processes in floodplain sediments of the Upper Colorado River Basin. Science of the Total Environment, 2017, 603-604, 663-675.	8.0	55

#	Article	IF	CITATIONS
37	The exceptionally stable cobalt(III)–desferrioxamine B complex. Marine Chemistry, 2009, 113, 114-122.	2.3	51
38	A Critical Review of the Physicochemical Impacts of Water Chemistry on Shale in Hydraulic Fracturing Systems. Environmental Science & Technology, 2021, 55, 1377-1394.	10.0	51
39	Structural Similarities between Biogenic Uraninites Produced by Phylogenetically and Metabolically Diverse Bacteria. Environmental Science & Technology, 2009, 43, 8295-8301.	10.0	50
40	Processes of Zinc Attenuation by Biogenic Manganese Oxides Forming in the Hyporheic Zone of Pinal Creek, Arizona. Environmental Science & Technology, 2014, 48, 2165-2172.	10.0	46
41	Thicknesses of Chemically Altered Zones in Shale Matrices Resulting from Interactions with Hydraulic Fracturing Fluid. Energy & Fuels, 2019, 33, 6878-6889.	5.1	46
42	Geochemical and mineralogical investigation of uranium in multi-element contaminated, organic-rich subsurface sediment. Applied Geochemistry, 2014, 42, 77-85.	3.0	40
43	Redox Fluctuations and Organic Complexation Govern Uranium Redistribution from U(IV)-Phosphate Minerals in a Mining-Polluted Wetland Soil, Brittany, France. Environmental Science & Technology, 2018, 52, 13099-13109.	10.0	40
44	Shale Kerogen: Hydraulic Fracturing Fluid Interactions and Contaminant Release. Energy & Fuels, 2018, 32, 8966-8977.	5.1	40
45	Complexation by Organic Matter Controls Uranium Mobility in Anoxic Sediments. Environmental Science & Technology, 2020, 54, 1493-1502.	10.0	37
46	Redox Heterogeneities Promote Thioarsenate Formation and Release into Groundwater from Low Arsenic Sediments. Environmental Science & Technology, 2020, 54, 3237-3244.	10.0	36
47	Redox Controls over the Stability of U(IV) in Floodplains of the Upper Colorado River Basin. Environmental Science & Technology, 2017, 51, 10954-10964.	10.0	33
48	Effect of Mn(II) on the Structure and Reactivity of Biogenic Uraninite. Environmental Science & Technology, 2009, 43, 6541-6547.	10.0	32
49	Uranium storage mechanisms in wet-dry redox cycled sediments. Water Research, 2019, 152, 251-263.	11.3	32
50	Uranium Association with Iron-Bearing Phases in Mill Tailings from Gunnar, Canada. Environmental Science & Technology, 2013, 47, 12695-12702.	10.0	31
51	Partitioning of uranyl between ferrihydrite and humic substances at acidic and circum-neutral pH. Geochimica Et Cosmochimica Acta, 2017, 215, 122-140.	3.9	31
52	Carbonate Facilitated Mobilization of Uranium from Lacustrine Sediments under Anoxic Conditions. Environmental Science & Technology, 2018, 52, 9615-9624.	10.0	29
53	Diverse ecophysiological adaptations of subsurface Thaumarchaeota in floodplain sediments revealed through genome-resolved metagenomics. ISME Journal, 2022, 16, 1140-1152.	9.8	28
54	Evaluating Chemical Extraction Techniques for the Determination of Uranium Oxidation State in Reduced Aquifer Sediments. Environmental Science & Technology, 2013, 47, 9225-9232.	10.0	27

#	Article	IF	CITATIONS
55	<mml:math <br="" xmlns:mml="http://www.w3.org/1998/Math/MathML">display="inline"><mml:mrow><mml:msub><mml:mrow><mml:mi>UO</mml:mi></mml:mrow><mml:mn>2Corrosion by Nonclassical Diffusion. Physical Review Letters, 2015, 114, 246103.</mml:mn></mml:msub></mml:mrow></mml:math>	ml: ml:א א <td>າml2ຄsub><!--</td--></td>	າm l2ຄ sub> </td
56	Reactive Transport Modeling of Shale–Fluid Interactions after Imbibition of Fracturing Fluids. Energy & Fuels, 2020, 34, 5511-5523.	5.1	25
57	Chemical and Reactive Transport Processes Associated with Hydraulic Fracturing of Unconventional Oil/Gas Shales. Chemical Reviews, 2022, 122, 9198-9263.	47.7	25
58	Long-Term in Situ Oxidation of Biogenic Uraninite in an Alluvial Aquifer: Impact of Dissolved Oxygen and Calcium. Environmental Science & Technology, 2015, 49, 7340-7347.	10.0	23
59	Oxidative Uranium Release from Anoxic Sediments under Diffusion-Limited Conditions. Environmental Science & Technology, 2017, 51, 11039-11047.	10.0	21
60	Diverse Thaumarchaeota Dominate Subsurface Ammonia-oxidizing Communities in Semi-arid Floodplains in the Western United States. Microbial Ecology, 2020, 80, 778-792.	2.8	19
61	Impact of Microbial Mn Oxidation on the Remobilization of Bioreduced U(IV). Environmental Science & Technology, 2013, 47, 3606-3613.	10.0	18
62	Uranium Immobilization and Nanofilm Formation on Magnesium-Rich Minerals. Environmental Science & Technology, 2016, 50, 3435-3443.	10.0	17
63	Calcium-Uranyl-Carbonato Species Kinetically Limit U(VI) Reduction by Fe(II) and Lead to U(V)-Bearing Ferrihydrite. Environmental Science & Technology, 2020, 54, 6021-6030.	10.0	17
64	Imaging Pyrite Oxidation and Barite Precipitation in Gas and Oil Shales. , 2018, , .		15
65	Experimental redox transformations of uranium phosphate minerals and mononuclear species in a contaminated wetland. Journal of Hazardous Materials, 2020, 384, 121362.	12.4	15
66	Isotopic Fingerprint of Uranium Accumulation and Redox Cycling in Floodplains of the Upper Colorado River Basin. Environmental Science & Technology, 2019, 53, 3399-3409.	10.0	14
67	Stability of Floodplain Subsurface Microbial Communities Through Seasonal Hydrological and Geochemical Cycles. Frontiers in Earth Science, 2020, 8, .	1.8	14
68	A Molecular Investigation of Soil Organic Carbon Composition across a Subalpine Catchment. Soil Systems, 2018, 2, 6.	2.6	13
69	Porewater Lead Concentrations Limited by Particulate Organic Matter Coupled With Ephemeral Iron(III) and Sulfide Phases during Redox Cycles Within Contaminated Floodplain Soils. Environmental Science & Technology, 2021, 55, 5878-5886.	10.0	13
70	Multiphysics Investigation of Geochemical Alterations in Marcellus Shale Using Reactive Core-Floods. Energy & Fuels, 2021, 35, 10733-10745.	5.1	13
71	FeS colloids – formation and mobilization pathways in natural waters. Environmental Science: Nano, 2020, 7, 2102-2116.	4.3	13
72	Oxidative Corrosion of the UO2 (001) Surface by Nonclassical Diffusion. Langmuir, 2017, 33, 13189-13196.	3.5	12

#	Article	IF	CITATIONS
73	Effects of Hydraulic Fracturing Fluid Chemistry on Shale Matrix Permeability. , 2018, , .		12
74	From legacy contamination to watershed systems science: a review of scientific insights and technologies developed through DOE-supported research in water and energy security. Environmental Research Letters, 2022, 17, 043004.	5.2	12
75	Barium Sources in Hydraulic Fracturing Systems and Chemical Controls on its Release into Solution. , 2018, , .		11
76	Diagenetic formation of uranium-silica polymers in lake sediments over 3,300 years. Proceedings of the National Academy of Sciences of the United States of America, 2021, 118, .	7.1	10
77	Chemical Speciation and Stability of Uranium in Unconventional Shales: Impact of Hydraulic Fracture Fluid. Environmental Science & Technology, 2020, 54, 7320-7329.	10.0	9
78	Geochemical Modeling of Iron (Hydr)oxide Scale Formation During Hydraulic Fracturing Operations. , 2019, , .		8
79	Simulated Aquifer Heterogeneity Leads to Enhanced Attenuation and Multiple Retention Processes of Zinc. Environmental Science & Technology, 2021, 55, 2939-2948.	10.0	8
80	Uranium(VI) attenuation in a carbonate-bearing oxic alluvial aquifer. Journal of Hazardous Materials, 2021, 412, 125089.	12.4	8
81	Export of Organic Carbon from Reduced Fine-Grained Zones Governs Biogeochemical Reactivity in a Simulated Aquifer. Environmental Science & Technology, 2022, 56, 2738-2746.	10.0	8
82	Strontium Behavior in Midland Basin Unconventional Reservoirs: The Importance of Base Fluids. , 2020, , .		7
83	Geochemical Modeling of Celestite (SrSO ₄) Precipitation and Reactive Transport in Shales. Environmental Science & Technology, 2022, 56, 4336-4344.	10.0	7
84	Global Sensitivity Analysis of a Reactive Transport Model for Mineral Scale Formation During Hydraulic Fracturing. Environmental Engineering Science, 2021, 38, 192-207.	1.6	6
85	Mineralogical and Porosity Alteration Following Fracture Fluid-Shale Reaction. , 2017, , .		5
86	Synchrotron X-ray Imaging of Element Transport Resulting from Unconventional Stimulation. , 2020, ,		5
87	<i>In Situ</i> Determination of Speciation and Local Structure of NaCl–SrCl ₂ and LiF–ZrF ₄ Molten Salts. Journal of Physical Chemistry B, 2022, 126, 1539-1550.	2.6	5
88	Trace Impurities Identified as Forensic Signatures in CMX-5 Fuel Pellets Using X-ray Spectroscopic Techniques. Analytical Chemistry, 2022, 94, 7084-7091.	6.5	4
89	A New Approach to Controlling Barite Scaling in Unconventional Systems. , 2019, , .		3
90	Controlling Strontium Scaling in the Permian Basin through Manipulation of Base Fluid Chemistry and Additives. , 2021, , .		3

6

#	Article	IF	CITATIONS
91	Synchrotron-based transmission x-ray microscopy for improved extraction in shale during hydraulic fracturing. Proceedings of SPIE, 2015, , .	0.8	2
92	Time-Lapse Acoustic Monitoring of Facture Alteration in Marcellus Shale. , 2020, , .		1
93	Impact of Acid–Base Stimulation Sequence on Mineral Stability for Tight/Impermeable Unconventional Carbonate-Rich Rocks: A Delaware Basin Case Study. Energy & Fuels, 2022, 36, 4746-4756.	5.1	1
94	Advancing Informational Gain from Synchrotron Techniques in Subsurface Science. Synchrotron Radiation News, 2019, 32, 24-26.	0.8	0
95	Acoustic velocity and permeability of acidized and propped fractures in shale. Geophysics, 2022, 87, MR13-MR24.	2.6	0